LANGMUIR

Species Distribution in Bicontinuous Phase Systems for Enhanced Oil Recovery Probed by Single-Sided NMR

Manuel I. Velasco,* Agustín Iborra, Juan M. Giussi, Omar Azzaroni, and Rodolfo H. Acosta

Read Online

ACCESS | Metrics & More | Article Recommendations | Supporting Information

ABSTRACT: Multiphase aqueous-organic systems where a bicontinuous phase is in equilibrium with an excess organic and aqueous phase find various applications in industry. These systems—also known as Winsor III—are complex not only for the different phases that develop therein but also because they are multicomponent systems. In this work, we explore for the first time the use of a benchtop low-field single-sided NMR to determine the species distribution in Winsor III systems. The proposed methodology provides information at macroscopic and microscopic levels. In particular, we show the use of single-sided NMR to determine the phases' dimensions and the species distribution in a polymer-based bicontinuous system. The phases' dimensions and limits can be resolved with micrometric precision and are indicative of the bicontinuous phase stability. The species distribution is determined by means of spatially resolved NMR relaxation and diffusion experiments. It was observed that the salinity of the aqueous phase also impacts the species distribution in the bicontinuous system. Experiments show that the additive and the polymer are mainly located in the bicontinuous phase. As the salinity of the aqueous phase increases, the amount of organic components in the bicontinuous phase decreases as a consequence of the species distribution in the system. This influences the total amount of recovered organic liquid from the organic phase. The information is obtained in a relatively fast experiment and is relevant to the system's possible applications, such as enhanced oil recovery (EOR). This methodology is not only circumscribed to its application in EOR but can also be applied to the study of any emulsion or microemulsion systems without sample size or geometry constraints.
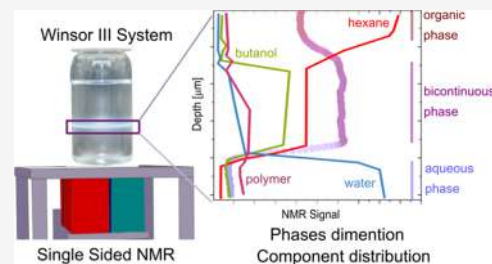
INTRODUCTION

Emulsions are systems in which two immiscible liquids are temporarily mixed homogeneously to produce a dispersion of one phase in the other.[1] The most effective strategy to inhibit phase separation is adding surfactants. Due to their amphiphilic nature, these entities are adsorbed at the interface and form a viscoelastic film around the disperse system, thus reducing the tendency to coalesce.[2] These systems play a crucial role in many processes such as controlled release drug delivery,[3] cosmetic industry,[4] bioseparations methods,[5] and fundamentally, in enhanced oil recovery (EOR).[6−9] Among the most remarkable properties of an emulsion are the type of emulsion, size, distribution of droplets, and system stability.

In the 1950s, Winsor[10] classified microemulsions by relating the interactions of adsorbed surfactant molecules at the interface with oil and water molecules in equilibrium. When the system involves a microemulsion in equilibrium with an excess phase, Winsor I and II systems are formed. A Winsor I system is an oil-in-water microemulsion with an upper excess organic phase. In Winsor II, the equilibrium is between a lower aqueous excess phase and a water-in-oil microemulsion. When the affinity of the surfactant molecules for the phases is similar, a triphasic system is formed. These systems are known as Winsor III and contain most of the surfactant with highly interconnected water and oil domains. In a Winsor III system, a bicontinuous microemulsion is in equilibrium with two

excess phases: an upper excess organic phase and a lower excess aqueous phase. When used for EOR, several factors affect the behavior of microemulsions under reservoir conditions; they include but are not limited to the class and molecular structure of the surfactant, temperature, salinity, solvent, pressure, and pH.[11] A critical aspect is the amphiphilic component selection since it directly affects the stability and behavior of the microemulsion.[12−14] We have previously designed and prepared amphiphilic copolymers to use as emulsifying agents that showed an adequate hydrophilic—lipophilic balance.[2,15]

Different techniques such as titration[16] and differential scanning calorimetry[17,18] (among others) are used to evaluate the composition in microemulsions. However, these methods are destructive, and the information collected is often limited to an average compound or composition. Nuclear magnetic resonance (NMR) has proven to help characterize the individual components of these bicontinuous systems. Most
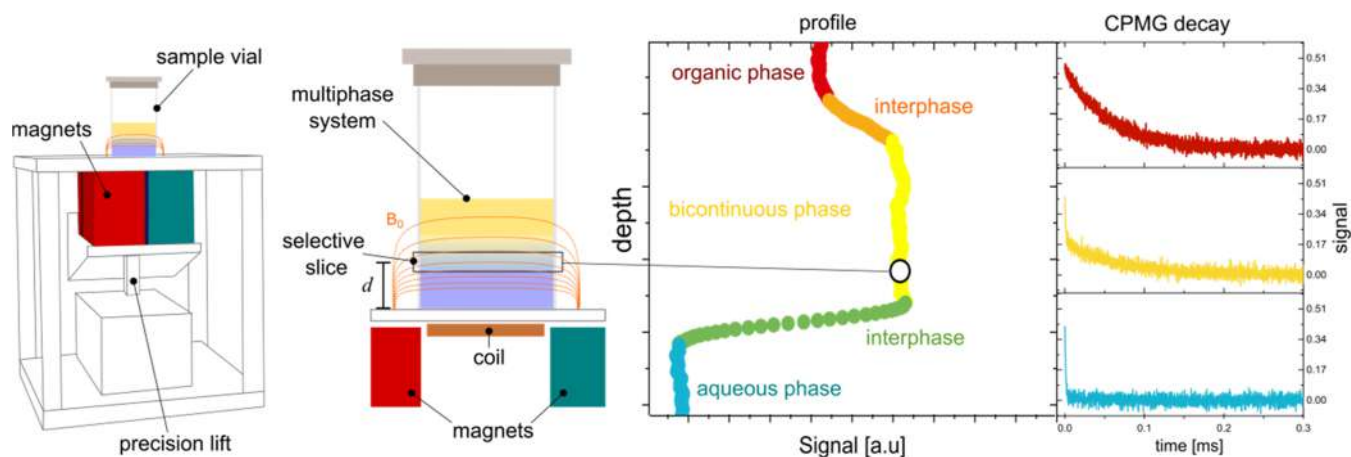
Figure 1. Schematic representation of the single-sided NMR-MOUSE showing the experimental setup, an acquired profile, and the detected signal decay during a Carr−Purcell−Meiboom−Gill (CPMG) pulse sequence.

of the studies report the use of this technique for structure elucidation or synthesis control.[19] However, the use of NMR to analyze multiphase and multicomponent systems has been less exploited.[20,21] One of the advantages of NMR is that it is suitable for studying optically opaque or turbid solutions, where other optical techniques may fail. For the particular study of microemulsions, most experiments use pulsed field gradient (PFG) pulse sequences to determine the self-diffusion coefficients of the components.[22−29]

In some cases, PFG is combined with NMRspectroscopy to further differentiate between species in a mixture.[30−33] In recent years, benchtop NMR has gained many users due to various factors. Not only do they have lower price and involve null maintenance costs but their operation modes are also easy that do not require an NMR expert and special laboratory requirements. Only a few reports used benchtop equipment to localize the components in a microemulsion,[34] determine diffusion coefficients,[35] monitor the oil saturation in a stone plug,[36] and study the emulsification kinetics.[37]

Single-sided NMR sensors combine surface radio frequency (RF) coils and open magnets to generate a sensitive slice external to the sensor and inside the sample under investigation.[38] This setup enables the study of arbitrarily sized objects in a noninvasive way since the sample lies outside the equipment. Since the NMR signal arises solely from the excited selective slice, the information provided is spatially resolved with typical depth resolutions in the range of 50−500 μm.[39,40] By changing the position of the sensitive slice, data from different parts of the sample is obtained; thus, different phases of the sample can be scanned. It has been widely used to study and characterize different systems, including rubber testing, cultural heritage, cementation, and gelatinization processes, among many others.[41−45]

In this work, we design, prepare, and characterize a bicontinuous phase based on an aqueous saline phase/*n*-hexane/LMA$_{60}$PEGMA$_{40}$/*n*-butanol using single-sided NMR methodologies adapted to the study of these systems. The copolymer synthesis was performed by reversible-addition fragmentation (RAF) chain-transfer polymerization. Using single-sided NMR, we developed a method for inspecting the system components as a function of the position. Since salinity significantly influences the system's capacity to recover organic fluids,[46−48] we use this relatively fast methodology to probe the system under different salinity conditions. We believe that

these results provide fundamental insights into the capabilities of emulsifying agents for their potential use in oil recovery and other applications, as well as the prospective use of single-sided NMR to characterize bicontinuous phases, microemulsions, and other colloidal systems.

■ EXPERIMENTAL SECTION

Polymer Synthesis. The polymerization mixture was prepared in a Schlenk flask by dissolving 8 g of poly(ethylene glycol) methyl ether methacrylate (Aldrich average M_n 500) and 6.12 g of lauryl methacrylate (Aldrich 96%) and purging with N$_2$ bubbling for 30 min. Afterward, 3.29 mg of 1,1′-azobis(cyclohexanecarbonitrile) (Aldrich 98%) and 41.6 mg of 4-cyano-4-(dodecylsulfanylthiocarbonyl) sulfanyl pentanoic acid (Aldrich 97%) were added predissolved in 1 mL of tetrahydrofuran. The flask was heated to 70 °C, and after 6 h, the reaction mixture was dissolved in tetrahydrofuran. The crude polymer was purified first by precipitation in *n*-hexane and then the precipitate was dissolved in water, and the dissolution was dialyzed and freeze-dried.

Sample Preparation. The samples are composed of an aqueous solution with different concentrations of salts (3, 5, and 7%), hexane as the organic phase, amphiphilic LMA$_{60}$PEGMA$_{40}$ polymer, and butanol as a cosolvent. The aqueous phase is prepared by dissolving CaCl$_2$ (11.5 g/L), MgCl$_2$ (11.8 g/L), Na$_2$SO$_4$ (0.5 g/L), and NaCl (38.5 g/L). Different aliquots of this solution are diluted in water to obtain the different salt concentrations (3, 5, and 7%) in the aqueous phase. Then, 240 μL of a 10% w/w solution of the polymer and 800 μL of butanol are added to 8 mL of the aqueous solution. Finally, 8 mL of hexane is gently added, and the tube is then rotated up and down to allow phase contact. After a resting period of a few minutes, the multiphase system is developed (see the Supporting Information). Since temperature affects the structure and stability of the bicontinuous phase,[13,49] the thermal sensitivity was tested. Systems showed stability at room temperature, and the triphasic structure is conserved below 40 °C. Before the measurement, a small part (approximately 1 mL) of the bottom aqueous phase is removed using a Pasteur glass pipette to ensure that the different phases can be monitored with the maximum penetration depth of the single-sided NMR sensor. The capped flask is placed directly on top of the equipment, and measurements are acquired at room temperature (Figure 1).

NMR Measurements. NMR measurements were carried out in a single-sided PM25 NMR-MOUSE (MObile Universal Surface Explorer) from Magritek GmbH, which operates at a resonance frequency of 12.99 MHz for ^{1}H nuclei and can detect signals of horizontal slices with an area of 4 × 4 cm^2 with a static magnetic field gradient of 7 T/m. The device was configured to achieve a maximum penetration depth of 10.6 mm and a resolution of 50 μm. Radio

frequency pulses of 9.5 μs with varying amplitude for the 90° and 180° flip angles were used in the different experiments.

The most standard technique for measuring the decay of time-domain signals in this type of device is with a multipulse, Carr−Purcell−Meiboom−Gill (CPMG) pulse sequence.[50,51] The intensity of the signal in a slice located at a distance d of the surface of the equipment (S_d) corresponding to the top of the echoes is described as

$$S_d(m\tau) = A(d)e^{\{-[(1/T_2)+1/12D(\gamma\tau G_0)^2]m\tau\}} \tag{1}$$

where T_2 is the transversal relaxation time, γ is the ^{1}H gyromagnetic ratio, G_0 is the magnetic field gradient intensity, τ is the echo time, m is the echo number, and D is the diffusion coefficient of the spin-bearing molecules. The coefficient $A(d)$ is proportional to the number of hydrogen nuclei in a sample slice located at depth d during the scanning. To obtain the full CPMG decays at specific values of d, different slices were detected, where 4000 echoes with an echo time τ = 120 μs were acquired with 16 averages to improve the signal-to-noise ratio. The echo time was chosen as a compromise between coil heating and experimental repetition time.[52] Equation 1 shows that signal attenuation due to molecular diffusion during the CPMG pulse sequence is produced. As each phase studied here has different diffusion coefficients, the effect of diffusion is included in the effective relaxation time, T_{2e}; therefore, the magnetization decay is considered as

$$S_d(t) = A(d)e^{-t/T_{2e}} \tag{2}$$

with $t = m\tau$.

Profile Acquisition. As the sensor can be repositioned to different d values, information from different slices may be obtained with a precision of 10 μm. Acquisition of the first data point in the CPMG decay provides a positional distribution of the sample or a one-dimensional (1D) image of the sample, where the intensity is related to the number of hydrogen nuclei per slice. This procedure is referred to as a profile acquisition. Additional contrast may be introduced by acquiring and adding a given number of echoes during the CPMG acquisition;[53] following eq 2, it can be observed that species with short relaxation times will have a reduced intensity compared to species with longer relaxation times. As our interest is mainly in the bicontinuous phase, the scanning depth was chosen between 10.4 and 5 mm, and 541 slices were measured using steps of 10 μm. The acquisition of a complete CPMG decay is more time-consuming, so to optimize the acquisition time of the profile, only 70 echoes were acquired with 16 scans. For comparison purposes, the relative value of d is referenced as zero to the last data point corresponding to the aqueous phase. A scheme of the experimental setup and typical signal response is shown in Figure 1 for the sample with a 3% of salt concentration.

Diffusion Measurements. Diffusion measurements were carried out using a stimulated echo (STE)[54] pulse sequence with CPMG detection. In the presence of a constant magnetic field gradient, the normalized signal attenuation is expressed as[38]

$$\ln\left(\frac{S_d(\tau_1, \tau_2)}{S_d(\tau_{1,min}, \tau_2)}\right) = -\gamma^2 G^2 \tau_1^2\left(\tau_2 + \frac{2}{3}\tau_1\right)D - \frac{2\tau_1}{T_2} - \frac{\tau_2}{T_1} \tag{3}$$

where the echo time was varied linearly from $\tau_{1,min}$ = 0.08 to $\tau_{1,max}$ = 1.25 ms to encode diffusion, while the storage time, τ_2, was fixed at 5 ms. For the CPMG detection, 10 echoes were coadded, and 128 scans were acquired for each τ_1 value. The CPMG echo train in the acquisition is used to improve the experiment's sensitivity.[38]

Diffusion−Relaxation Correlation. Diffusion-T_2 correlation experiments were performed using the same STE sequence. The timings τ_1 were linearly varied in 50 steps from 0.08 to 1.25 ms, while τ_2 was fixed at 5 ms. For the CPMG detection, 8000 echoes and 32 scans were acquired for each τ_1 value with a repetition time of 4.9 s.

Numerical Inversion of Data Decays. In complex systems where several components contribute to a signal decay, either for transverse magnetization during a CPMG pulse sequence or due to diffusion in an STE pulse sequence, a combination of different decay

rates drives the signal evolution. For transverse magnetization, eq 2 may be rewritten as

$$S_d(t) = \sum_{i=1}^{n} A_i(d)e^{\{-t/T_{2e,i}\}} \tag{4}$$

where n represents the number of relaxation rates present in the system. Numerical inverse Laplace processing is usually carried out to obtain the distribution of relaxation times, that is, the factors A_i related to the decay constants $T_{2e,i}$ employing Contin or Upen methods.[55,56] For diffusion measurements, the last two terms in eq 3 are not considered in this work; these can be neglected for long T_1 and T_2 values compared with experimental times, which is not necessarily the case for all of the involved species. This data processing does not render the real diffusion coefficient values but an effective one, D_e. The signal attenuation due to diffusion in an STE pulse sequence is then considered to be

$$S_d(b) = \sum_{j=1}^{l} B_j(d)e^{\{-bD_{e,j}\}} \tag{5}$$

where the b value is $\gamma^2 G^2 \tau_1^2\left(\tau_2 + \frac{2}{3}\tau_1\right)$. After the introduction of the first two-dimensional (2D) algorithm for data inversion introduced by Venkataramanan et al.,[57] many strategies for the obtention of 2D relaxation maps were introduced. In this work, we use the algorithm introduced by Teal and Eccles[58] with a reconstruction matrix of 100 × 100 points and an adapted version for 1D data inversion.

■ RESULTS AND DISCUSSION

Determination of the Bicontinuous Phase Thickness. To determine the phases' dimensions, profile experiments were performed for the different samples. In particular, the thickness of the bicontinuous phase is relevant with the view to its applications in EOR, since it is necessary to determine the amount of organic matter recovered by the microemulsion. This aspect will be discussed in more detail in the following section. In addition, it can be used to monitor the stability of the microemulsion as a function of time.[14] Different profiles can be measured as a function of time to monitor the development of the different phases (see the Supporting Information). Once the three phases have been formed, the profiles can help investigate whether the system is stable over time. If the profiles coincide, then the microemulsion is stable over that period. It is worth mentioning that the relaxation and diffusion parameters obtained by single-sided NMR (those obtained from eqs 4 and 5) can also be indicative of the system's stability.[59] The experiments reported in this work are performed on stable systems.

As shown in Figure 1 for the sample with 3% of salt concentration, the transverse magnetization decays of each phase are clearly distinguished, as the three different phases have significantly different signal intensities and relaxation decay rates. These differences can be attributed to several factors. The first is salinity, which is responsible for the fast decay of water in the aqueous and in bicontinuous phases.[60] On the other hand, since salts have very low or negligible solubility in the organic phase, the decay is unaffected. The other relevant factor is the density of ^{1}H in each phase, which is reflected in the CPMG signal intensity.

It is then possible to use these differences as a contrast in the profile acquisition. The profile data points are built by adding the first 70 echoes of the CPMG decay. Since the phases have different decays, the addition of the 70 first echoes of the aqueous phase renders a lower value than the sum of those of the organic phase. In this way, it is possible to acquire a T_2-

weighted profile of the samples that provides the dimensions of the different phases. In particular, we focused our attention on the bicontinuous phase, and Figure 2 shows the profiles
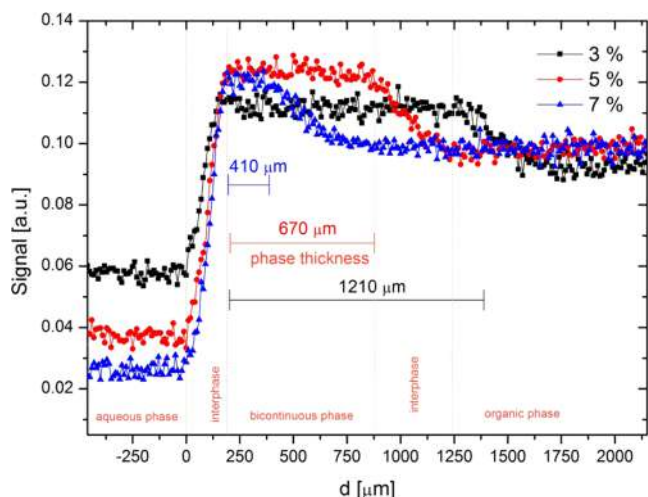
Figure 2. Profiles of the three studied samples. The dotted lines show the phases determined for the 5% salt concentration sample.

obtained for the samples for various salt concentrations. The data at low d values correspond to the aqueous phase. As previously mentioned, the salinity is high, and consequently, the decays are fast, leading to a low amount of signal. In the bicontinuous phase, a steep increase in the signal is observed as the bicontinuous phase has a much longer T_2 relaxation value than the aqueous one, together with higher proton density. This fact is related to the dual composition of the phase, which incorporates material from the upper organic layer. Different samples render different values since the formed phases vary in composition, as discussed in the next section. For higher values of d, the signal intensity decays as the interphase between the bicontinuous and organic phases is reached. It can also be seen that for the three different samples, the aqueous-bicontinuous interface limit is sharper than the interface between the bicontinuous and the organic phase. Finally, the purely organic phase is reached, and the signal reaches a constant value higher than the one corresponding to the aqueous phase and lower than the bicontinuous one.

From each profile, the thickness of the bicontinuous phase can be determined simply by subtracting the values of d, as seen in Figure 2. The determined values are 1210, 670, and 410 μm for 3, 5, and 7% of salinity, respectively. It can be seen that as the salinity of the aqueous phase increases, the bicontinuous phase thickness decreases since different salt concentrations affect the balance of interactions between the polar components of the mixture. The different ions produce a screening effect between the polymer polar groups and the water molecules, which reduces the interaction on the water side of the amphiphile.[61] The same effect affects the interactions between the polymer and the butanol. Bicontinuous microemulsion only occurs when the interactions between the amphiphilic polymer and the oil and water phases are similar.[10] The resulting arrangement can satisfy both affinities so that the equal dislikes for oil and water are canceled. By increasing the salinity, the previously mentioned ion screening effect is also increased and alters the distribution of all components across the sample. The difference in the

composition leads to variation in the bicontinuous microemulsion structure.[62,63] Consequently, the interfacial tensions are modified, and the macroscopic thicknesses of the bicontinuous phases are altered.[64,65]

Species Distribution among the Phases. Through relaxation and diffusion experiments at different depths, the different phases' compositions can be explored. The CPMG decays obtained in the profiling experiment were optimized to determine the phase dimension in a rapid experiment. However, since only a few echoes are acquired, the resulting decays are insufficient to determine the species distribution using eq 4. Once the phase dimensions and positions have been determined, the selective slice of the NMR-MOUSE can be placed in specific values of d, and more time-consuming experiments can be performed to determine the sample's composition, acquiring a complete CPMG decay. The assignation of each component's relaxation and diffusion coefficient was done using a more straightforward reference solution. Readers are referred to the Supporting Information for a detailed discussion of the assignation procedure. The resulting values of $T_{2,e}$ and D_e are summarized in Table S1 (Supporting Information).

Positioning the sensor in the center of each phase, a $D-T_2$ experiment is used to determine the different components present in these sensitive volumes. Figure 3 shows the result of
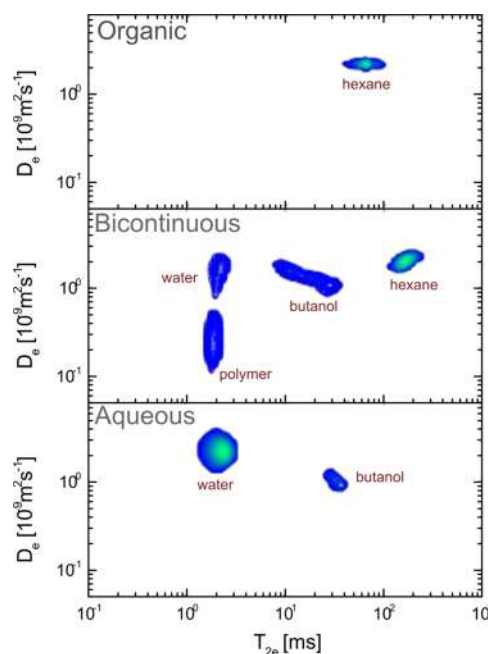
Figure 3. $D-T_2$ map of the different phases in the 3% salinity sample.

$D-T_2$ maps for the 3% salinity sample. Comparing the obtained values of $T_{2,e}$ and D_e with the reference samples, it can be stated that the organic phase is composed of hexane (Figure 3, upper panel) and the aqueous phase with the salt solution and butanol (Figure 3, lower panel). The composition of the bicontinuous phase is clearly more complex, and multiple components are shown on the map (Figure 3, middle panel).

Based on the initial profiles and the result of the 2D experiments, different values of depth were chosen to explore the composition of the samples (Figure 4). The first value (lower d) is representative of the composition of the pure aqueous phase. Then, increasing the d value, a few points were
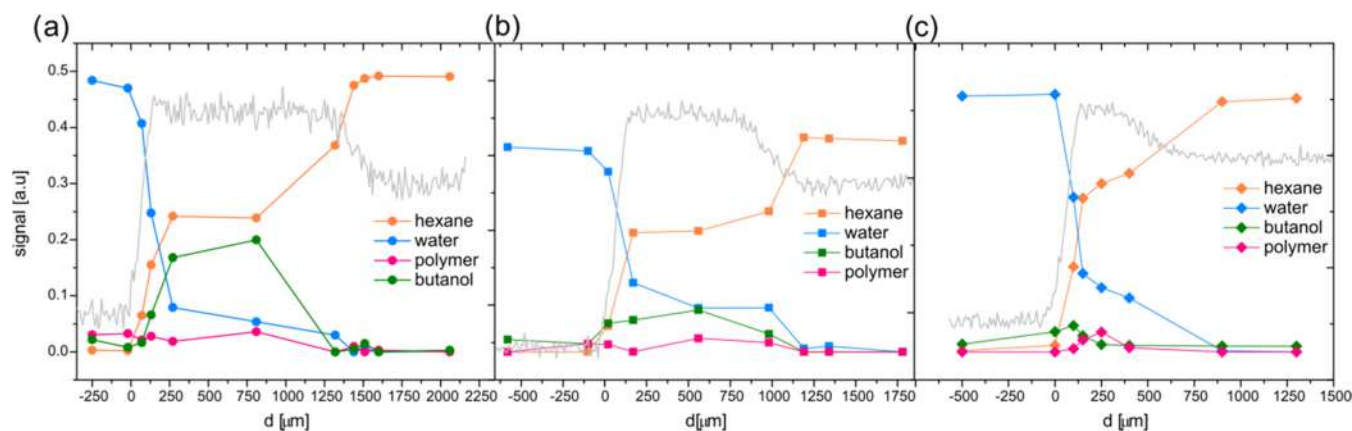
Figure 4. species distribution determined by NMR in the samples of (a) 3%, (b) 5%, and (c) 7%.

acquired to study the characteristics of the interphase between the aqueous and the bicontinuous phases, attempting to sample the borders and middle of the interface as well. Two heights were selected as representative of the bicontinuous phase in the 3 and 5% salinity samples. As the 7% salinity sample has a very thin bicontinuous phase, only one height is measured. Finally, some point explores the limits and middle of the interphase between the bicontinuous and organic phases, and one point represents the purely organic phase.

Figure 4 shows the species distribution for the 3, 5, and 7% salt concentrations. The species distribution is built from the CPMG decays. For a single slice, the CPMG signal is composed of the contributions of each constituent's decay. The different T_{2e} values are distinctive enough to be fitted from the decay. As previously stated, the assignation of each T_{2e} value was based on simpler standard solutions (see the Supporting Information).

In the bicontinuous structure, the polymer monolayer is self-organized to some highly connected surface of the cubic symmetry, dividing the oil and aqueous channels.[24] Since the amphiphilic polymer is composed of hydrophobic and hydrophilic side chains, it is expected that it presents a "pancake state," where the primary backbone is on the surface, and its hydrophilic and hydrophobic tails stick out into the water/oil domains, respectively.[22,66] It is important to note that in this situation, water and polymer exhibit a very similar T_{2e} value because their relaxation is affected by the ions in the aqueous phase. Consequently, the signal decay is swift, and the CPMG cannot efficiently sense two different decays. However, since the D_e values are different, the composition of the polymer can be determined. The salinity does not affect the more polar molecules with no exchangeable protons, so the CPMG easily distinguishes their relaxation value.

As shown in Figure 4, in the bicontinuous phase, water and hexane coexist. However, the proportion between hexane and water in the central points of the bicontinuous phases is different. Therefore, the NMR data shown can be used to monitor how the different components partition in the three phases. It can be seen that for the 5 and 7% solutions, the amount of hexane is 2.6 and 2.7, respectively. In contrast, the 3% formulation reaches a 4.5 value. The difference in the composition can be attributed to the species distribution. The 3% formulation is the one that shows a higher proportion of alcohol in the bicontinuous phase. The amount of butanol diminishes as the salinity is increased. It can also be observed that an increase in the salinity reduces the water solubilization

into the middle phase due to a reduction in the water–microemulsion interfacial activity.[67] A closer inspection of the polymer distribution shows that it is also affected by the salinity of the aqueous phase. In the 3% sample, these molecules are mainly distributed in the aqueous and bicontinuous phases. However, as salinity increases, the distribution shows that the polymer tends to reside in the bicontinuous and organic phases. As previously mentioned, the increase in salinity of the aqueous phase changes the balance of interactions in the system. The transition of the polymer from the bicontinuous phase to the organic phase is then forced, and the systems shifts from a Winsor III to a Winsor II. It has been previously reported that changes in the salt, water, and additive amounts produce differences in the microemulsion structure sizes.[62,63] The differences observed by NMR also support the results shown by Hayes et al., where the interphase of Winsor III systems undergoes gradual structural transition and composition in the vertical direction.[68]

It is worth noting that in such a complex formulation, the distribution of different species is not the consequence of a single parameter. Furthermore, an increase in the local number of additives and the salinity affects the dimensions and topology of the molecule's ensemble in the bicontinuous phase, leading to a variation in the total amount of hexane that can be hosted in the channels. The NMR data can also be used to determine the total amount of hexane recovered in the three samples. As previously discussed, the sample with higher salinity exhibits more hexane in the bicontinuous phase. However, the thickness of the phase is the lowest. Therefore, multiplying the thickness of the bicontinuous phase by the hexane fraction determined renders the total amount of hexane that the system can solubilize in the bicontinuous equilibrium state (Figure 5). This amount is proportional to the recovery factor or solubilization parameter usually employed in EOR studies.[69] The data can be obtained in a single fast NMR experiment. It is worth mentioning that the acquisition of spatially resolved data is not exclusive to single-sided equipment, so a similar analysis can be performed with other NMR types of equipment with the necessary hardware to acquire spatially resolved data.

■ CONCLUSIONS

Single-sided NMR proves to be a valuable tool for studying bicontinuous systems. This technique can provide the spatial distribution of the different components of the studied bicontinuous systems, as well as macroscopic parameters,
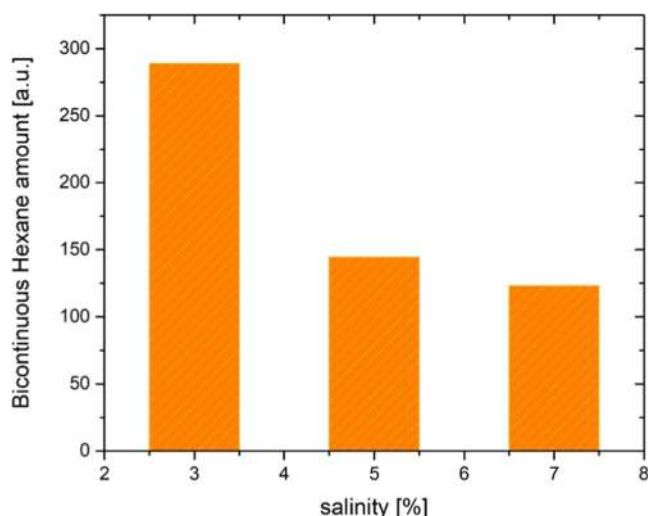
Figure 5. Amount of hexane in the bicontinuous phase for the three studied samples.

such as the phases and interphase dimensions. It does not require the use of deuterated solvents and may be helpful in analyzing not only Winsor III systems but also other microemulsions. The results show that the salinity of the aqueous phase affects not only the phases' dimensions but also their composition. Consequently, it has an important impact on the amount of recovered organic liquid from the organic phase. This parameter is very relevant, given the system's possible applications. The relaxation and diffusion values of the components were also determined, and the differences observed can be interpreted as a consequence of changes in the interactions between them.

ASSOCIATED CONTENT

Supporting Information

The Supporting Information is available free of charge at https://pubs.acs.org/doi/10.1021/acs.langmuir.2c02302.

> Synthesis and characterization of the polymer, stability of the system, detailed report and assignation of the different relaxation and diffusion coefficient values, and the methodology for the construction of the species distribution plots (PDF)

AUTHOR INFORMATION

Corresponding Author

Manuel I. Velasco − *Facultad de Matemática, Astronomía, Física y Computación, Universidad Nacional de Córdoba, Córdoba X5000HUA, Argentina; CONICET, Instituto de Física Enrique Gaviola (IFEG), Córdoba X5000HUA, Argentina;* orcid.org/0000-0003-1500-4672; Email: mvelasco@unc.edu.ar

Authors

Agustín Iborra − *Instituto de Investigaciones Fisicoquímicas Teóricas y Aplicadas (INIFTA), Departamento de Química, Facultad de Ciencias Exactas, Universidad Nacional de La Plata, CONICET, 1900 La Plata, Argentina; YPF Tecnología S.A., Buenos Aires 1925, Argentina*

Juan M. Giussi − *YPF Tecnología S.A., Buenos Aires 1925, Argentina*

Omar Azzaroni − *Instituto de Investigaciones Fisicoquímicas Teóricas y Aplicadas (INIFTA), Departamento de Química, Facultad de Ciencias Exactas, Universidad Nacional de La Plata, CONICET, 1900 La Plata, Argentina;* orcid.org/0000-0002-5098-0612

Rodolfo H. Acosta − *Facultad de Matemática, Astronomía, Física y Computación, Universidad Nacional de Córdoba, Córdoba X5000HUA, Argentina; CONICET, Instituto de Física Enrique Gaviola (IFEG), Córdoba X5000HUA, Argentina;* orcid.org/0000-0003-3945-8273

Complete contact information is available at:
https://pubs.acs.org/10.1021/acs.langmuir.2c02302

Notes

The authors declare no competing financial interest.

ACKNOWLEDGMENTS

REFERENCES

(1) Salager, J.-L.; Rondón, M.; Tolosa, L.; Pizzino, A.; Bullon, J. Emulsion Formulation Engineering for the Practitioner. *Encycl. Surf. Colloid Sci.* **2010**, *1*, 1−16.

(2) Iborra, A.; Díaz, G.; López, D.; Giussi, J. M.; Azzaroni, O. Copolymer Based on Lauryl Methacrylate and Poly(Ethylene Glycol) Methyl Ether Methacrylate as Amphiphilic Macrosurfactant: Synthesis, Characterization and Their Application as Dispersing Agent for Carbon Nanotubes. *Eur. Polym. J.* **2017**, *87*, 308−317.

(3) Batrakova, E. V.; Kabanov, A. V. Pluronic Block Copolymers: Evolution of Drug Delivery Concept from Inert Nanocarriers to Biological Response Modifiers. *J. Controlled Release* **2008**, *130*, 98−106.

(4) Fakhravar, Z.; Ebrahimnejad, P.; Daraee, H.; Akbarzadeh, A. Nanoliposomes: Synthesis Methods and Applications in Cosmetics. *J. Cosmet. Laser Ther.* **2016**, *18*, 174−181.

(5) Gomez del Rio, J. A.; Hayes, D. G. Protein Extraction by Winsor-III Microemulsion Systems. *Biotechnol. Prog.* **2011**, *27*, 1091−1100.

(6) Spildo, K.; Sun, L.; Djurhuus, K.; Skauge, A. A Strategy for Low Cost, Effective Surfactant Injection. *J. Pet. Sci. Eng.* **2014**, *117*, 8−14.

(7) Lake, L. W.; Schmidt, R. L.; Venuto, P. B. A Niche for Enhanced Oil Recovery in the 1990s. *Oilf. Rev.* **1992**, *4*, 55−61.

(8) Al-Mjeni, R.; Arora, S.; Cherukupalli, P.; Van Wunnik, J.; Edwards, J.; Felber, B. J.; Gurpinar, O.; Hirasaki, G. J.; Miller, C. A.; Jackson, C.; Kristensen, M. R.; Lim, F.; Ramamoorthy, R. Has the Time Come for EOR? *Oilf. Rev.* **2010**, *22*, 16−35.

(9) Pal, N.; Mandal, A. Oil Recovery Mechanisms of Pickering Nanoemulsions Stabilized by Surfactant-Polymer-Nanoparticle Assemblies: A Versatile Surface Energies' Approach. *Fuel* **2020**, *276*, No. 118138.

(10) Winsor, P. A. Binary and Multicomponent Solutions of Amphiphilic Compounds. Solubilization and the Formation, Structure, and Theoretical Significance of Liquid Crystalline Solutions. *Chem. Rev.* **1968**, *68*, 1−40.

(11) Mahboob, A.; Kalam, S.; Kamal, M. S.; Hussain, S. M. S.; Solling, T. EOR Perspective of Microemulsions: A Review. *J. Pet. Sci. Eng.* **2022**, No. 109312.

(12) Pal, N.; Kumar, N.; Mandal, A. Stabilization of Dispersed Oil Droplets in Nanoemulsions by Synergistic Effects of the Gemini Surfactant, PHPA Polymer, and Silica Nanoparticle. *Langmuir* **2019**, *35*, 2655−2667.

(13) Kabalnov, A.; Weers, J. Macroemulsion Stability within the Winsor III Region: Theory versus Experiment. *Langmuir* **1996**, *12*, 1931−1935.

(14) Rastogi, P.; Kaisare, N. S.; Basavaraj, M. G. Diesel Emulsion Fuels with Ultralong Stability. *Energy and Fuels* **2019**, *33*, 12227−12235.

(15) Iborra, A.; Salvatierra, L.; Giussi, J. M.; Azzaroni, O. Synthesis of Lauryl Methacrylate and Poly(Ethylene Glycol) Methyl Ether Methacrylate Copolymers with Tunable Microstructure and Emulsifying Properties. *Eur. Polym. J.* **2019**, *116*, 117−125.

(16) Fukumoto, A.; Dalmazzone, C.; Frot, D.; Barré, L.; Noïk, C. Investigation on Physical Properties and Morphologies of Microemulsions Formed with Sodium Dodecyl Benzenesulfonate, Isobutanol, Brine, and Decane, Using Several Experimental Techniques. *Energy Fuels* **2016**, *30*, 4690−4698.

(17) Fukumoto, A.; Dalmazzone, C.; Frot, D.; Barré, L.; Noïk, C. Characterization of Complex Crude Oil Microemulsions-DSC Contribution. *Oil Gas Sci. Technol. − Rev. d'IFP Energies Nouv.* **2018**, *73*, 3.

(18) Garti, N.; Aserin, A.; Tiunova, I.; Fanun, M. A DSC Study of Water Behavior in Water-in-Oil Microemulsions Stabilized by Sucrose Esters and Butanol. *Colloids Surf., A* **2000**, *170*, 1−18.

(19) Pal, N.; Saxena, N.; Mandal, A. Equilibrium and Dynamic Adsorption of Gemini Surfactants with Different Spacer Lengths at Oil/Aqueous Interfaces. *Colloids Surf., A* **2017**, *533*, 20−32.

(20) Gröger, S.; Rittig, F.; Stallmach, F.; Almdal, K.; Štěpánek, P.; Papadakis, C. M. A Pulsed Field Gradient Nuclear Magnetic Resonance Study of a Ternary Homopolymer/Diblock Copolymer Blend in the Bicontinuous Microemulsion Phase. *J. Chem. Phys.* **2002**, *117*, 396−406.

(21) Söderman, O.; Henriksson, U. NMR Studies of Bicontinuous Liquid Crystalline Phases of Cubic Symmetry: Interpretation of Frequency-Dependent Relaxation Rates. *Langmuir* **2020**, *36*, 5927−5934.

(22) Nilsson, M.; Söderman, O.; Johansson, I. The Effect of Polymers on the Phase Behavior of Balanced Microemulsions: Diblock-Copolymer and Comb-Polymers. *Colloid Polym. Sci.* **2006**, *284*, 1229−1241.

(23) Lindman, B.; Kamenka, N.; Kathopoulis, T. M.; Brun, B.; Nilsson, P. G. Translational Diffusion and Solution Structure of Microemulsions. *J. Phys. Chem. A* **1980**, *84*, 2485−2490.

(24) Zuev, Y. F.; Vylegzhanina, N. N.; Idiyatullin, B. Z.; Mirgorodskaya, A. B. Effects of Solubilized Dodecylamine on the Microstructure of Cetylpyridinium Bromide-n-Butanol-Hexane-Water System Studied by Pulsed-Gradient Spin Echo NMR and ESR Spin Label Methods. *Appl. Magn. Reson.* **2003**, *25*, 65−77.

(25) Söderman, O.; Nydén, M. NMR in Microemulsions. NMR Translational Diffusion Studies of a Model Microemulsion. *Colloids Surf., A* **1999**, *158*, 273−280.

(26) Vermeir, L.; Balcaen, M.; Sabatino, P.; Dewettinck, K.; Van der Meeren, P. Influence of Molecular Exchange on the Enclosed Water Volume Fraction of W/O/W Double Emulsions as Determined by Low-Resolution NMR Diffusometry and T2-Relaxometry. *Colloids Surf., A* **2014**, *456*, 129−138.

(27) Law, S. J.; Britton, M. M. Sizing of Reverse Micelles in Microemulsions Using NMR Measurements of Diffusion. *Langmuir* **2012**, *28*, 11699−11706.

(28) D'Agostino, C.; Mitchell, J.; Mantle, M. D.; Gladden, L. F. Interpretation of NMR Relaxation as a Tool for Characterising the Adsorption Strength of Liquids inside Porous Materials. *Chem. - Eur. J.* **2014**, *20*, 13009−13015.

(29) Mitchell, J.; Lyons, K.; Howe, A. M.; Clarke, A. Viscoelastic Polymer Flows and Elastic Turbulence in Three-Dimensional Porous Structures. *Soft Matter* **2016**, *12*, 460−468.

(30) Colafemmina, G.; Mateos, H.; Palazzo, G. Diffusion NMR Studies of Complex Liquid Formulations. *Curr. Opin. Colloid Interface Sci.* **2020**, *48*, 109−120.

(31) St Thomas, C.; Elizalde, L. E.; Regalado, E. J.; De Jesús-Téllez, M. A.; Festag, G.; Schubert, U. S.; Guerrero-Sánchez, C. Under-

standing the Influence of Chemical Structure and Length of Hydrophobic Blocks on the Rheological Properties of Associative Copolymers. *Eur. Polym. J.* **2021**, *143*, No. 110190.

(32) Mills, A. J.; Wilkie, J.; Britton, M. M. NMR and Molecular Dynamics Study of the Size, Shape, and Composition of Reverse Micelles in a Cetyltrimethylammonium Bromide (CTAB)/n-Hexane/Pentanol/Water Microemulsion. *J. Phys. Chem. B* **2014**, *118*, 10767−10775.

(33) Zuev, Y. F.; Mirgorodskaya, A. B.; Idiyatullin, B. Z. Structural Properties of Microheterogeneous Surfactant-Based Catalytic Systems: Multicomponent Self-Diffusion NMR Approach. *Appl. Magn. Reson.* **2004**, *27*, 489−500.

(34) Herrera, D.; Chevalier, T.; Fleury, M.; Dalmazzone, C. Quantification of Microemulsion Systems Using Low-Field T1-Weighted Imaging. *Magn. Reson. Imaging* **2021**, *83*, 160−168.

(35) Pradilla, D.; Barrera, A.; Sætran, M. G.; Sørland, G.; Alvarez, O. Mechanisms of Physical Stabilization of Concentrated Water-In-Oil Emulsions Probed by Pulse Field Gradient Nuclear Magnetic Resonance and Rheology through a Multiscale Approach. *Langmuir* **2018**, *34*, 9489−9499.

(36) Howe, A. M.; Clarke, A.; Mitchell, J.; Staniland, J.; Hawkes, L.; Whalan, C. Visualising Surfactant Enhanced Oil Recovery. *Colloids Surf., A* **2015**, *480*, 449−461.

(37) Herrera, D.; Chevalier, T.; Frot, D.; Barré, L.; Drelich, A.; Pezron, I.; Dalmazzone, C. Monitoring the Formation Kinetics of a Bicontinuous Microemulsion. *J. Colloid Interface Sci.* **2022**, *609*, 200−211.

(38) Casanova, F.; Perlo, J.; Blümich, B.; Hürlimann, M. D.; Demas, V.; Franck, J. M.; Reimer, J. A.; Pines, A.; Danieli, E. D.; Kolz, J.; Felder, J. *Single-Sided NMR*; Casanova, F.; Perlo, J.; Blümich, B., Eds.; Springer Berlin Heidelberg: Berlin, Heidelberg, 2011.

(39) Eidmann, G.; Savelsberg, R.; et al. The NMR MOUSE, a Mobile Universal Surface Explorer. *J. Magn. Reson., Ser. A* **1996**, *122*, 104−109.

(40) Blümich, B.; Anferov, V.; Anferova, S.; Klein, M.; Fechete, R. An NMR-MOUSE for Analysis of Thin Objects. *Macromol. Mater. Eng.* **2003**, *288*, 312−317.

(41) Blümich, B.; Casanova, F.; Perlo, J.; Anferova, S.; Anferov, V.; Kremer, K.; Goga, N.; Kupferschläger, K.; Adams, M. Advances of Unilateral Mobile NMR in Nondestructive Materials Testing. *Magn. Reson. Imaging* **2005**, *23*, 197−201.

(42) Rehorn, C.; Blümich, B. Cultural Heritage Studies with Mobile NMR. *Angew. Chem., Int. Ed.* **2018**, *57*, 7304−7312.

(43) Goga, N. O.; Pirnău, A.; Szabo, L.; Smeets, R.; Riediger, D.; Cozar, O.; Blümich, B. Mobile NMR: Applications to Materials and Biomedicine. *J. Optoelectron. Adv. Mater.* **2006**, *8*, 1430−1434.

(44) Danieli, E.; Blümich, B. Single-Sided Magnetic Resonance Profiling in Biological and Materials Science. *J. Magn. Reson.* **2013**, *229*, 142−154.

(45) Ghoshal, S.; Mattea, C.; Denner, P.; Stapf, S. Heterogeneities in Gelatin Film Formation Using Single-Sided NMR. *J. Phys. Chem. B* **2010**, *114*, 16356−16363.

(46) Zhu, Z.; Kou, H.; Zhang, Z.; Wang, Y.; Wan, H. Performance and Mechanisms of Enhanced Oil Recovery via Amphiphilic Polymer Flooding in High Salinity Reservoir. *Pet. Sci. Technol.* **2022**, 1−11.

(47) Yang, H.; Zhang, H.; Zheng, W.; Li, X.; Wang, F.; Li, X.; Zhang, D.; Turtabayev, S.; Kang, W. Research on Synthesis and Salt Thickening Behavior of a Binary Copolymer Amphiphilic Polymer. *J. Pet. Sci. Eng.* **2021**, *204*, No. 108713.

(48) Wang, F.; Yang, H.; Li, M.; Kang, X.; Zhang, X.; Zhang, H.; et al. Study on Stabilization of Emulsion Formed by the Supramolecular System of Amphiphilic Polymer and Sodium Polyacrylic Acid. *J. Mol. Liq.* **2020**, *314*, No. 113644.

(49) Morales, D.; Gutiérrez, J. M.; García-Celma, M. J.; Solans, Y. C. A Study of the Relation between Bicontinuous Microemulsions and Oil/Water Nano-Emulsion Formation. *Langmuir* **2003**, *19*, 7196−7200.

(50) Meiboom, S.; Gill, D. Modified Spin-Echo Method for Measuring Nuclear Relaxation Times. *Rev. Sci. Instrum.* **1958**, *29*, 688.

(51) Carr, H. Y.; Purcell, E. M. Effects of Diffusion on Free Precession in Nuclear Magnetic Resonance Experiments. *Phys. Rev.* **1954**, *94*, 630.

(52) Silletta, E. V.; Velasco, M. I.; Monti, G. A.; Acosta, R. H. Comparison of Experimental Times in T1-D and D-T2 Correlation Experiments in Single-Sided NMR. *J. Magn. Reson.* **2022**, *334*, No. 107112.

(53) Perlo, J.; Casanova, F.; Blümich, B. Profiles with Microscopic Resolution by Single-Sided NMR. *J. Magn. Reson.* **2005**, *176*, 64−70.

(54) Stejskal, E. O.; Tanner, J. E. Spin Diffusion Measurements: Spin Echoes in the Presence of a Time-Dependent Field Gradient. *J. Chem. Phys.* **1965**, *42*, 288−292.

(55) Provencher, S. W. A Constrained Regularization Method for Inverting Data Represented by Linear Algebraic or Integral Equations. *Comput. Phys. Commun.* **1982**, *27*, 213−227.

(56) Borgia, G. C.; Brown, R. J. S.; Fantazzini, P. Uniform-Penalty Inversion of Multiexponential Decay Data: II. Data Spacing, T2 Data, Systematic Data Errors, and Diagnostics. *J. Magn. Reson.* **2000**, *147*, 273−285.

(57) Venkataramanan, L.; Song, Y. Q.; Hürlimann, M. D. Solving Fredholm Integrals of the First Kind with Tensor Product Structure in 2 and 2.5 Dimensions. *IEEE Trans. Signal Process.* **2002**, *50*, 1017−1026.

(58) Teal, P. D.; Eccles, C. Adaptive Truncation of Matrix Decompositions and Efficient Estimation of NMR Relaxation Distributions. *Inverse Probl.* **2015**, *31*, No. 045010.

(59) Malmborg, C.; Topgaard, D.; Söderman, O. Diffusion in an Inhomogeneous System: NMR Studies of Diffusion in Highly Concentrated Emulsions. *J. Colloid Interface Sci.* **2003**, *263*, 270−276.

(60) Kwak, H. T.; Zhang, G.; Chen, S.; Atlas, B. In *The Effects of Salt Type and Salinity on Formation Water Viscosity and NMR Responses*, Proceedings of the international symposium of the Society of Core Analysts, 2005; 1−13.

(61) Salager, J.-L.; Forgiarini, A. M.; Bullón, J. Surfactant Formulation Guidelines to Reach an Ultralow Interfacial Tension for Enhanced Oil Recovery. In *Topics in Colloidal Aggregation and Interfacial Phenomena*, Garcia-Sucre, M.; Lozsan, C. M. G.-S.; Aileen, L.; Castellanos-Suarez, A.; Toro-Mendoza, J., Eds.; Research Signpost: Kerala, 2012; pp 125−160.

(62) Mulder, M.; Li, X. X.; Nazim, M. M.; Dalgliesh, R. M.; Tian, B.; Buijse, M.; van Wunnik, J.; Bouwman, W. G. Systematically Quantifying Oil−Water Microemulsion Structures Using (Spin-Echo) Small Angle Neutron Scattering. *Colloids Surf., A* **2019**, *575*, 166−175.

(63) Marquez, R.; Forgiarini, A. M.; Langevin, D.; Salager, J. L. Instability of Emulsions Made with Surfactant-Oil-Water Systems at Optimum Formulation with Ultralow Interfacial Tension. *Langmuir* **2018**, *34*, 9252−9263.

(64) Reed, R.; Healy, R. Some Physicochemical Aspects of Microemulsion Flooding: A Review. In *Improved Oil Recovery by Surfactant and Polymer Flooding*; Schecheter, R. S.; Shah, D. O., Eds.; Academic Press, 1977; pp 383−347.

(65) Bourrel, M.; Chambu, C.; Schechter, R. S.; Wade, W. H. The Topology of Phase Boundaries for Oil/Brine/Surfactant Systems and Its Relationship to Oil Recovery. *Soc. Pet. Eng. J.* **1982**, *22*, 28−36.

(66) Indrani, C. H. V. A.; Lipowsky, R. Membranes with Anchored Polymers at the Adsorption Transition. *Europhys. Lett.* **1996**, *36*, 491−496.

(67) Pal, N.; Saxena, N.; Mandal, A. Phase Behavior, Solubilization, and Phase Transition of a Microemulsion System Stabilized by a Novel Surfactant Synthesized from Castor Oil. *J. Chem. Eng. Data* **2017**, *62*, 1278−1291.

(68) Hayes, D. G.; Pingali, S. V.; O'Neill, H. M.; Urban, V. S.; Ye, R. Observation of a Structural Gradient in Winsor-III Microemulsion Systems. *Soft Matter* **2018**, *14*, 5270−5276.

(69) Pal, N.; Kumar, S.; Bera, A.; Mandal, A. Phase Behaviour and Characterization of Microemulsion Stabilized by a Novel Synthesized Surfactant: Implications for Enhanced Oil Recovery. *Fuel* **2019**, *235*, 995−1009.

📖 **Recommended by ACS**